

## Characteristic findings of magnetic resonance imaging (MRI) and computed tomography (CT) for severe chronic laminitis in a Thoroughbred horse

Kazutaka YAMADA<sup>1\*</sup>, Tomohiro INUI<sup>2</sup>, Megumi ITOH<sup>2</sup>, Masashi YANAGAWA<sup>2</sup>, Fumio SATO<sup>3</sup>, Masataka TOMINARI<sup>3</sup>, Fumiaki MIZOBE<sup>4</sup>, Miori KISHIMOTO<sup>5</sup> and Naoki SASAKI<sup>2</sup>

<sup>1</sup>Azabu University, Kanagawa 252-5201, Japan

<sup>2</sup>Obihiro University of Agriculture and Veterinary Medicine, Hokkaido 080-8555, Japan

<sup>3</sup>Hidaka Training and Research Center, Japan Racing Association, Hokkaido 057-0171, Japan

<sup>4</sup>Race Horse Hospital, Ritto Training Center, Japan Racing Association, Shiga 520-3085, Japan

<sup>5</sup>Tokyo University of Agriculture and Technology, Tokyo 183-8538, Japan

---

*A Thoroughbred horse with severe chronic laminitis of both forelimbs was evaluated on the same day with magnetic resonance imaging (MRI) and computed tomography (CT). Both MRI and CT revealed loss of the dorsal aspect of the cortical bone of the 3rd phalanx and sclerosis. CT reflected the status of the horny layer and bone of the affected feet, while MRI depicted inflammation of the lamellar corium, together with tendon edema. On the 3-dimensional CT venogram, vessels were visualized in both the right and left forelimbs, although there was a difference in the vasculature of the coronary plexus and circumflex vessels between the right and left forelimbs. A combination of both MRI and CT provides detailed information regarding pathological conditions.*

**Key words:** *computed tomography (CT), laminitis, magnetic resonance imaging (MRI), venogram*

---

**J. Equine Sci.**  
**Vol. 28, No. 3**  
**pp. 105–110, 2017**

Diagnosis of laminitis is based upon a history of lameness in combination with physical abnormalities, including increased digital pulse, hoof wall heat, and characteristic findings on radiography. Laminitis often accompanies separation of the 3rd phalanx (P3), leading to displacement of the bone. Therefore, the rotation of P3 could be used as an indicator of the severity and prognosis of laminitis. However, there have only been a limited number of reports on evaluation of laminitis using magnetic resonance imaging (MRI), most of which have been the studies in cadaver limbs [1, 8]. Here, we describe our experience of evaluating a living case of chronic laminitis by using both MRI and computed tomography (CT) on the same day.

A 6-year-old Thoroughbred mare with a body weight

of 443 kg and body condition score based on Texas A&M University Equine Body Condition Score of 3, presented increased bilateral forelimb hoof temperature, prominent digital pulse, and a history of severe lameness for 25 months (Fig. 1). This horse had been treated with shoeing therapy. Radiography revealed rotation of P3 along with hoof wall separation, and the right forelimb seemed to be more severely affected compared with the left one. The horse underwent general anesthesia, and MRI was performed with an open gantry 0.4 Tesla magnetic field strength unit (APERTO Lucent, Hitachi, Tokyo, Japan) at the Veterinary Medical Teaching Hospital, Obihiro University of Agriculture and Veterinary Medicine. The horse was positioned in right lateral recumbency on the MRI patient table, each forelimb was placed in a human knee radiofrequency coil, and then sagittal T2-weighted images (Fast Spin Echo sequence; TR, 3,700 msec; TE, 100 msec; and slice thickness of 3.5 mm) and T1-weighted images (Spin Echo sequence; TR, 330 msec; TE, 20 msec; and slice thickness of 3.5 mm) were obtained. Following MRI, the horse was moved from the MRI examination room to a CT examination room. The horse was positioned in left lateral recumbency on the CT patient

---

Received: March 22, 2017

Accepted: May 30, 2017

\*Corresponding author. e-mail: kyamada@azabu-u.ac.jp

©2017 Japanese Society of Equine Science

This is an open-access article distributed under the terms of the Creative Commons Attribution Non-Commercial No Derivatives (by-nc-nd) License. (CC-BY-NC-ND 4.0: <https://creativecommons.org/licenses/by-nc-nd/4.0/>)



**Fig. 1.** Appearance of a Thoroughbred horse with chronic laminitis.

table, and CT images were subsequently obtained with a 16-row multidetector CT (Aquilion LB, Toshiba, Tokyo, Japan) by tube voltage of 135 kV, tube current of 250 mA, and slice thickness of 0.5 mm. Multi-planar reconstructed sagittal images were acquired using an image-processing workstation (VirtualPlace, Aze, Tokyo, Japan). Following the first CT scan, a tourniquet was applied to the fetlock joint, and the lateral palmar digital vein was catheterized as described previously [12]. Immediately after injection of 30 ml of iohexol (140 mgI/ml), the CT venogram was scanned, and a 3-dimensional (3D) venogram was made using an image-processing workstation.

In the left forelimb, there was moderate joint fluid distension in the distal interphalangeal joint capsule (Fig. 2a), a heterogeneous signal intensity in the laminar corium (Fig. 2b), a wavy dorsal aspect of the laminar corium (Fig. 2c), loss of the dorsal aspect of the cortical bone of P3 (Fig. 2d), and an increased signal intensity extending through the deep digital flexor tendon (Fig. 2e). In the right limb, which was also severely affected, there was reduced amount of fluid in the distal interphalangeal joint capsule (Fig. 3a), a high signal intensity in the dorsal cortex of the extensor process (Fig. 3b), a heterogeneous signal intensity in the laminar corium (Fig. 3c), and an increased signal intensity extending through the deep digital flexor tendon (Fig. 3d). Also, sclerosis (Fig. 3e) was imaged as an area of low signal intensity on MRI [9, 13], whereas it was imaged as an area of high density on CT. Hoof wall separations were identified

on CT (Fig. 3f) but not on MRI because of lower proton density in the hoof. Both MRI and CT revealed loss of the cortex bone and sclerosis, and CT was able to generate images that reflected the physical status of the affected hooves, including lamellar separation, while MRI was able to depict inflammation of the laminar corium together with tendon edema. MRI was superior to CT in detecting soft tissue changes. There was an area of low signal intensity in both the T1-weighted images and T2-weighted images in the distal interphalangeal joint capsule (Fig. 4a), which suggested chronic hemorrhage. There was also an area of heterogeneous signal intensity in the periopic corium (Fig. 4b). MRI was able to detect sclerosis but not bone marrow edema. Fat-suppressed images, which reflect the water content of spongy bone related to bone marrow edema, were not scanned in this study [10]. In chronic laminitis cases like this horse, it is presumed that inflammation within the hoof capsule is sustained for a long period of time, which may indicate that the condition could be evaluated using a short tau inversion recovery sequence. There was a difference in the volume of P3 when comparing the right ( $53.7 \text{ ml}^3$ ) and left ( $63.1 \text{ ml}^3$ ) sides in volume rendering 3D images measured by an image-processing workstation (Fig. 5). This difference revealed the degree of bony erosion of P3 as a result of chronic laminitis [3]. Volumetric measurement can be performed using CT, making it possible to perform quantitative evaluation.

Dyson *et al.* previously reported MRI findings using



**Fig. 2.** Mid-sagittal section in the left forelimb (left, MRI; center, CT; right, radiograph). There was moderate joint fluid distention in the distal interphalangeal joint capsule (a), a heterogeneous signal intensity in the lamellar corium (b), a wavy dorsal aspect of the lamellar corium (c), loss of the dorsal aspect of the cortical bone of the 3rd phalanx (d), and an increased signal intensity extending through the deep digital flexor tendon (e).



**Fig. 3.** Mid-sagittal section in the right forelimb (left, MRI; center, CT; right, radiograph). There was a reduced amount of fluid in the distal interphalangeal joint capsule (a), a high signal intensity in the dorsal cortex in the extensor process (b), a heterogeneous signal intensity in the lamellar corium (c), and an increased signal intensity extending through the deep digital flexor tendon (d). Sclerosis (e) was evident as an area of low signal intensity on MRI and an area of high density on CT. Hoof wall separation that was identifiable on CT (f) but not on MRI.

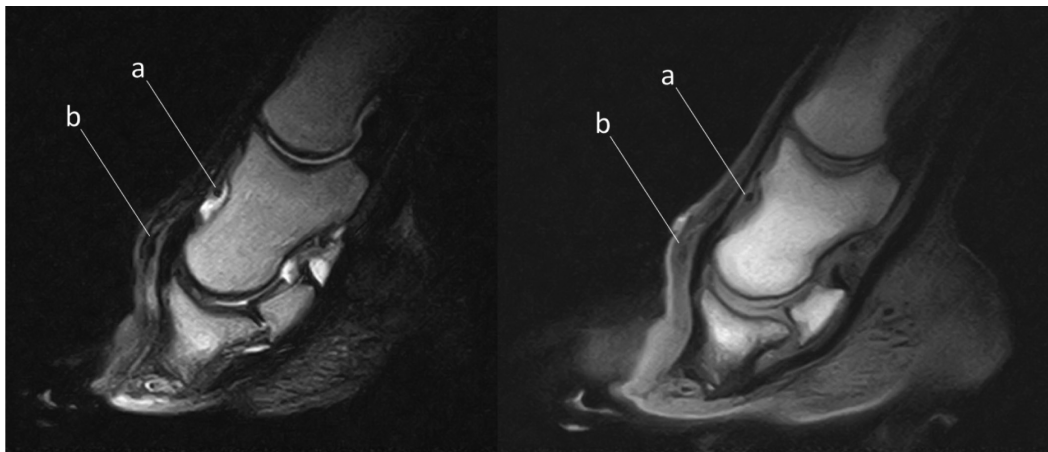


**Fig. 4.** Mid-sagittal section in the right forelimb (left, T2-weighted image; right, T1-weighted image). There was an area of low signal intensity in both the T1-weighted image and T2-weighted image in the distal interphalangeal joint capsule (a) and a heterogeneous signal intensity in the periosteal corium (b).

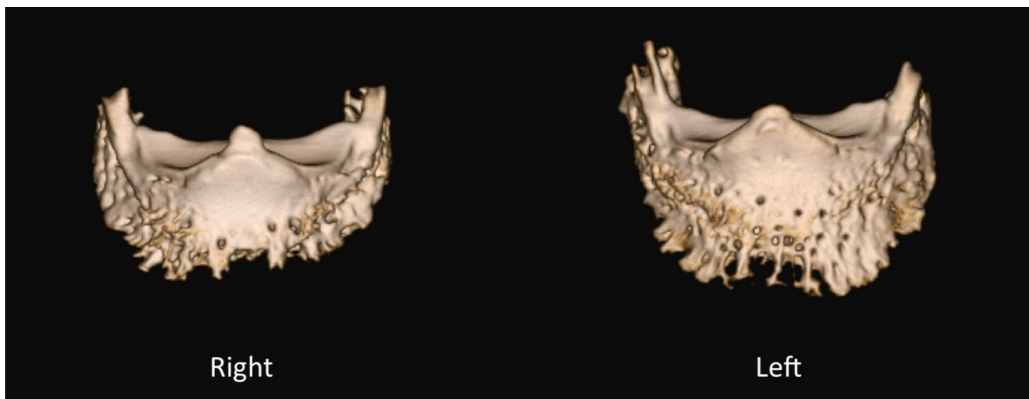


**Fig. 5.** Extracted 3-dimensional 3rd phalanx. The measured volume was 53.7 cm<sup>3</sup> in the right limb and 63.1 cm<sup>3</sup> in the left.

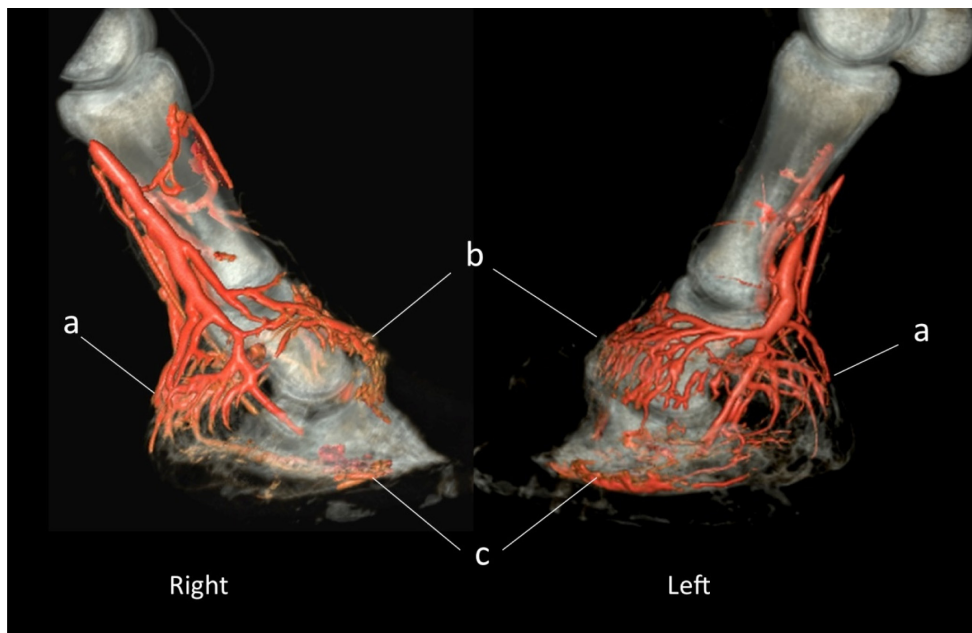


**Fig. 6.** Three-dimensional venogram (lateromedial view). Heel vessels were observed in both the right and left forelimbs (a), but there was a difference in the vasculature of the coronary plexus (b) and circumflex vessels (c) between the right and left forelimbs. The right limb showed more reduction than the left.

a 1.5 Tesla magnetic field MRI in 15 living horses [2]; in the present study, we used a 0.4 Tesla magnetic field. As the signal to noise ratio depends on the strength of the magnetic field, high magnetic field MRI confers an advantage over low magnetic field MRI in terms of image quality. In general, high magnetic field MRI has a small gantry, although the open gantry MRI used in this current case may require less labor for in positioning a horse in the magnet gantry. Standing MRI (sMRI) with a low magnetic field, which has the advantage of not requiring general anesthesia, was first introduced in 2005, and it has now become

widespread [5–7]. To the best of the authors' knowledge, no literature is available regarding specific investigations of live horses with laminitis using sMRI. Because of its low magnetic field, an sMRI would require a relatively long scan time. Laminitis often involves severe pain, indicating the difficulty in continuing to bear weight on the affected limb during a scan.

In the 3D venogram, heel vessels were visualized in both the right and left forelimbs (Fig. 6a), although there was a difference in the vasculature of the coronary plexus (Fig. 6b) and circumflex vessels (Fig. 6c) between the right

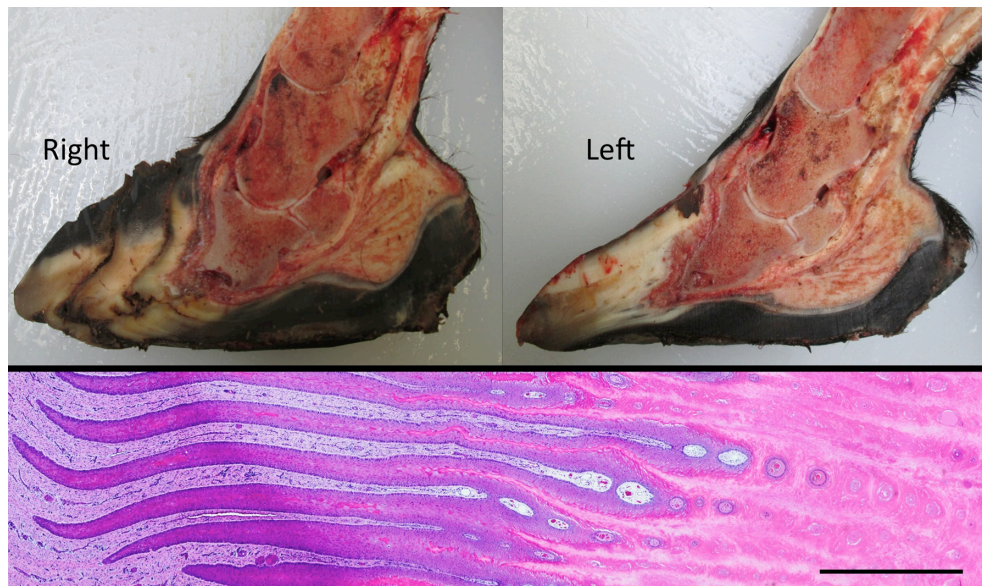


**Fig. 7.** Gross examination of the lamellar layer of the medium hoof wall in a sagittal section and histopathology. The bony deformity in the sagittal section was consistent with both MRI and CT. An ectopic white band tissue, an abnormal horny structure called a lamellar wedge, was continuously observed in the regenerated epidermal lamina (Hematoxylin-eosin stain, bar=1 mm).

and left limbs. The vasculature in the right limb was more reduced than that in the left, which was consistent with the degree of laminitis. While the same amount of contrast agent was injected into the digital vein, the right digital vein was larger than the left one. This might suggest that the total vessel volume in the right limb was smaller than that in the left one. Dorsal lamellar vessels were defective in both limbs, so we considered that there was a lack of dorsal lamellar vessels in both limbs. There are two additional possibilities for the lack of dorsal lamellar vessels. One is a defective hoof mechanism; that is, capability of the blood pumping mechanism in the hoof may have been reduced due to the horse lying recumbent on the CT patient table and therefore the limbs not being weight bearing. The second is a technical factor such as spatial resolution, which represents a limitation of the CT technique, and may have affected the ability to accurately determine whether or not there was a lack of vessels in the dorsal lamellar vessels. Radiographic venogram is often used to evaluate laminitis in clinical fields, and the spatial resolution of a radiograph is far superior to that of a CT venogram. While a radiographic venogram is a projection image, a 3D venogram allows us to easily understand the appearance of the vasculature. Importantly, the venogram would indicate a “blood pool” and not absolute “blood flow”. The contrast agent injected into the digital veins results in retrograde filling of the

arteries, and the contrast agent in the vessel is static rather than flowing. We suggest that the anatomical distribution of the contrast agent may be related to its perfusion, but it is necessary to have further discussion the clinical significance of venogram. Authors believed that evaluation of blood flow would require a dynamic contrast-enhanced CT [4, 11]. As the injection of an appropriate systemic dose of intravenous contrast agent into a horse is impractical due to the large volume requirement, a peripheral artery injection should be performed.

Immediately after MRI and CT, this case was clinically diagnosed with severe chronic laminitis and determined to have a poor prognosis, and the horse was euthanized without recovery from anesthesia. In gross sagittal sections, the bony deformity was consistent on MRI and CT. On histopathological examination, the dermis-epidermis was almost flat. An ectopic white band tissue, an abnormal horny structure called a lamellar wedge, was continuously observed on the regenerated epidermal lamina. Laminitis was confirmed by pathological examination (Fig. 7).

This represents the first report of both MRI and CT in a living case with chronic laminitis. When veterinarians have access to both MRI and CT, the combination of these two advanced techniques can help them acquire detailed information regarding underlying pathological conditions.

## Acknowledgments

The authors are grateful to Dr. Yoshiharu Ueno at the Hidaka Training and Research Center of the Japan Racing Association, Dr. Takanori Ueno at the Equine Research Institute of the Japan Racing Association, and Dr. Atsutoshi Kuwano at the Japan Farriery Association for technical assistance in pathological examination.

## References

1. Arble, J.B., Mattoon, J.S., Drost, W.T., Weisbrode, S.E., Wassenaar, P.A., Pan, X., Hunt, R.J., and Belknap, J.K. 2009. Magnetic resonance imaging of the initial active stage of equine laminitis at 4.7 T. *Vet. Radiol. Ultrasound* **50**: 3–12. [[Medline](#)] [[CrossRef](#)]
2. Dyson, S., Murray, R., Schramme, M., and Branch, M. 2003. Magnetic resonance imaging of the equine foot: 15 horses. *Equine Vet. J.* **35**: 18–26. [[Medline](#)] [[CrossRef](#)]
3. Engiles, J.B., Galantino-Homer, H.L., Boston, R., McDonald, D., Dishowitz, M., and Hankenson, K.D. 2015. Osteopathology in the equine distal phalanx associated with the development and progression of laminitis. *Vet. Pathol.* **52**: 928–944. [[Medline](#)] [[CrossRef](#)]
4. Kruger, E.F., Puchalski, S.M., Pollard, R.E., Galuppo, L.D., Hornof, W.J., and Wisner, E.R. 2008. Measurement of equine laminar blood flow and vascular permeability by use of dynamic contrast-enhanced computed tomography. *Am. J. Vet. Res.* **69**: 371–377. [[Medline](#)] [[CrossRef](#)]
5. Mair, T.S. 2005. Magnetic resonance imaging of the distal limb of the standing horse. *Equine Vet. Educ.* **17**: 74–78. [[CrossRef](#)]
6. Mair, T.S., and Linnenkohl, W. 2012. Low-field magnetic resonance imaging of keratomas of the hoof wall. *Equine Vet. Educ.* **24**: 459–468. [[CrossRef](#)]
7. Mizobe, F., Okada, J., Shinzaki, Y., Nomura, M., Kato, T., Yamada, K., and Spriet, M. 2016. Use of standing low-field magnetic resonance imaging to assess oblique distal sesamoidean ligament desmitis in three Thoroughbred racehorses. *J. Vet. Med. Sci.* **78**: 1475–1480. [[Medline](#)] [[CrossRef](#)]
8. Murray, R.C., Dyson, S.J., Schramme, M.C., Branch, M., and Woods, S. 2003. Magnetic resonance imaging of the equine digit with chronic laminitis. *Vet. Radiol. Ultrasound* **44**: 609–617. [[Medline](#)] [[CrossRef](#)]
9. Olive, J., Mair, T.S., and Charles, B. 2009. Use of standing low-field magnetic resonance imaging to diagnose middle phalanx bone marrow lesions in horses. *Equine Vet. Educ.* **21**: 116–123. [[CrossRef](#)]
10. Powell, S.E., Ramzan, P.H.L., Head, M.J., Shepherd, M.C., Baldwin, G.I., and Steven, W.N. 2010. Standing magnetic resonance imaging detection of bone marrow oedema-type signal pattern associated with subcarpal pain in 8 racehorses: a prospective study. *Equine Vet. J.* **42**: 10–17. [[Medline](#)] [[CrossRef](#)]
11. Puchalski, S.M., Galuppo, L.D., Hornof, W.J., and Wisner, E.R. 2007. Intraarterial contrast-enhanced computed tomography of the equine distal extremity. *Vet. Radiol. Ultrasound* **48**: 21–29. [[Medline](#)] [[CrossRef](#)]
12. Redden, R.F. 2001. A technique for performing digital venography in the standing horse. *Equine Vet. Educ.* **13**: 128–134. [[CrossRef](#)]
13. Sherlock, C.E., Mair, T.S., and Ter Braake, F. 2009. Osseous lesions in the metacarpo(tarso)phalangeal joint diagnosed using low-field magnetic resonance imaging in standing horses. *Vet. Radiol. Ultrasound* **50**: 13–20. [[Medline](#)] [[CrossRef](#)]